NILU TR: 6/90

NILU TR : 6/90
REFERENCE : Q-303
DATE : JUNE 1990
ISBN : 82-425-0126-2

RESEARCH AND DEVELOPMENT WITHIN THE LOCAL AIR POLLUTION GROUP AT NILU

ANNUAL REPORT 1989

Edited by
B. Sivertsen

NILU

NORSK INSTITUTT FOR LUFTFORSKNING
Norwegian Institute For Air Research
POSTBOKS 64 — N-2001 LILLESTRØM — NORWAY

SUMMARY

The research and development carried out by the local air pollution group at NILU is 1989 was mainly linked to air pollution modelling.

Models for various kinds of applications has been developed and is steadily being improved. Models have been a main tool of the group for estimating the environmental impact of emissions from existing sources, from new sources and due to changes in emissions. Dispersion models directly linked to air quality surveillance programmes have proved to be a powerful tool in explaining and improving measurement data. A variety of dispersion models for applications on different scales in space and time is thus available in the NILU model library.

During 1989 the development and improvement of the dispersion models at NILU included:

- An operative dispersion model directly linked to hourly meteorological input data
- A mesoscale puff trajectory model included NO_x chemistry and wet deposition
- A better system for traffic emissions and dispersion calculations
- Estimates of emissions and dispersion at road tunnel outlets
- Better description of the vertical dispersion of air pollutants in urban and suburban areas, with special emphasis on stable low wind conditions
- Improved model performance through the introduction of statistical optimization procedures linked to measurement data and model results.

CONTENTS

RESEARCH AND DEVELOPMENT WITHIN THE LOCAL AIR POLLUTION GROUP AT NILU

ANNUAL REPORT 1989

1 INTRODUCTION

The local air pollution group at NILU is undertaking research and development both as part of external projects and within the NILU internal research projects, mainly based upon grants from the Ministry of Environment.

A major part of the development during 1989 was linked to air pollution modelling. Models of different kinds for a variety of problems has always been the main tool of the group for performing consequence analysis and environmental impact statements. One important effort accomplished during 1989 was to link statistical optimization procedures to source oriented dispersion models in order to improve the performance of the model. This work was carried out with data from the Grenland health study. NO_x chemistry and wet deposition was also included in a mesoscale model, Improvements of road tunnel modelling and air pollution models for complete road and street systems were established during 1989. Modelling of airport impact including emissions from moving aeroplanes was also initiated in 1989.

Some of the development projects are briefly presented by the responsible research scientists below. The numbers in parantheses refer to NILU project numbers.

2 IMPROVEMENT OF AN OPERATIVE DISPERSION MODEL (E-8301)

Trond Bøhler

A method for calculating dispersion of plumes in the atmospheric boundary layer has been adapted to the NILU computer. The theoretical background was published in several articles by S.E. Gryning (Risø), A.A. Holtslag (KNMI). J.S. Irwin (EPA) and B. Sivertsen (NILU).

The atmospheric boundary layer is divided into a number of regimes defined by the scaling parameters z/h and h/L where z, h and L are the plume height, mixing height and Monin-Obukov length, respectively (Figure 1).

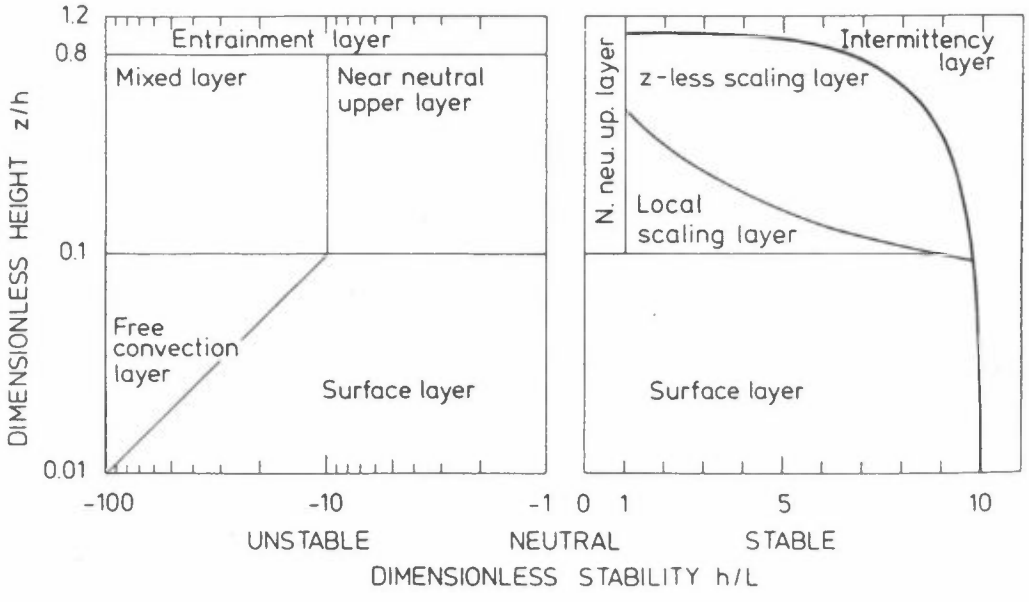

Figure 1: The scaling regions of the atmospheric boundary layer, shown as function of the dimensionless height z/h and the stability parameter h/L.

For each regime the model gives the crosswind-integrated concentrations at the ground for releases from a continuous point source. The method is limited to horizontally homogeneous conditions and travel distances less than 10 km.

Generally the vertical concentration profile is assumed to be other than Gaussian, while the lateral is always Gaussian. The method has been evaluated against tracer experiments showing good agreement and better than was predicted using traditional Gaussian plume model.

The model development at NILU will continue in 1990 with improvement of the "metprocessor", documentation of the model and further comparisons between measurements and predictions.

3 A MESOSCALE PUFF-TRAJECTORY MODEL WITH NO_x CHEMISTRY (E-8812)

Svein Knudsen

The project contains a further development of the EPA-model INPUFF. The Inpuff model is a mesoscale puff-trajectory model. The handbook by Peterson explains the EPA version. The model has been converted to run on a ND-500 mainframe computer. The model has been expanded to take into account NO_x chemistry. The NO_x chemistry includes 5 reactions. The reactions are:

R1: $NO_2 + h\nu \rightarrow NO + O_3$, $0 - 6.2\ 10^{-3}$

R2: $O_3 + NO \rightarrow NO_2 + O_2$, $2.1 + 10^{-12}\ e^{-1450/T}$

R3: $2NO + O_2 \rightarrow 2NO_2$, $1.5 * 10^{-40}\ e^{1780/T}$

R4: $O_3 + NO_2 \rightarrow NO_3^- + O_2$, $1.2 * 10^{-13}\ e^{-2450/T}$

The chemical numerical equation is treated with a time step of 5 s. Each puff is a well mixed ellipsoid of 2δ radius in each direction.

Within this ellipside the chemical reactions are taking place. The different NO_x components are then spread by the gaussian distribution to calculate the concentrations of NO, NO_2, and NO_3^-.

The model can also calculate the wet deposition from a NO_x-plume on an hourly basis. The model has been tested for gas power plant plumes where the NO_3^- wet deposition was calculated.

The model development is not finished. The model will be tested against another model "PLUME" (Hov, 1981) to validate the NO_x chemistry.

The chemical part of the model also needs some refinement on the diffusion and mixing. The chemical finite difference model by Hov has been made operative.

REFERENCES

Hov, Ø. and Isaksen, I.S.A. (1981) Generation of secondary pollutants in a power plant plume: A model study. Atmospheric Environment Vol. 15, No. 10/11, pp. 2367-2376.

Peterson, W.B. and Lavdas, L.G. (1986) Inpuff 2.0 - A multiple source Gaussian Puff Dispersion Algorithm. User's Guide. Atmospheric Sciences Research laboratory Office of Research and Development. Research Triangle Park, NC. EPA-600/8-86/024. NTIS PB 86-242 450.

4 ESTIMATES OF AIR QUALITY AROUND ROAD SYSTEMS (E-8948)

Frederick Gram

A series of programmes has been developed to estimate air quality from road traffic. The programmes are based upon a standard definition of a traffic data file with all relevant parameters for further calculations. The road system consists of links between traffic nodes, with data on traffic densities and speeds on each link. The traffic data may be calculated from sub models named: TRIPS, CONTROM or EMMA. In addition the model needs information of the slope and width of the link, percentage of diesel cars, cold starts, the number of households adjacent to the link, and the positions of each node.

The different sub programmes are:

Sted-KOMB-TRAF

Combines the data from all different sources, substitutes all missing data with data from NBB. (Nordisk Beregnings-metode for Bilavgasser), and produces a standard traffic file. Sted-KOMB-TRAF is a programme which is tailored for each new region.

GATE-UTSL

Calculates the emissions of CO and NO_x along each road link, from estimated data on the traffic work.

RUTE-UTSL

Calculates the emissions of CO and NO_x within grid squares of 500 m x 500 m or 1 km x 1 km. It also estimates the total traffic work within the grid. The emission data may be used to calculate fuel consumption and CO_2-emissions.

TRAF-KONS

Combines the emissions from one link and the link in the opposite direction. It calculates street concentrations according to NBB and concentrations along open roads according to a modified Stanford model. The concentrations are calculated from

$$[CO] = [CO]_{street} + [CO]_{region}$$

$$[NO_2] = a * [NO_x]_{street} + [NO_x] + [O_3]_{region} + [NO_2]_{region}$$

TRAF-EKSP

Calculates the number of persons which are exposed for concentrations above different limits from regional population distribution fields and from information of the number of households along the streets.

VRI-PLOT

Produces different types of plots of the road system, f.ex. concentrations with different colour codes.

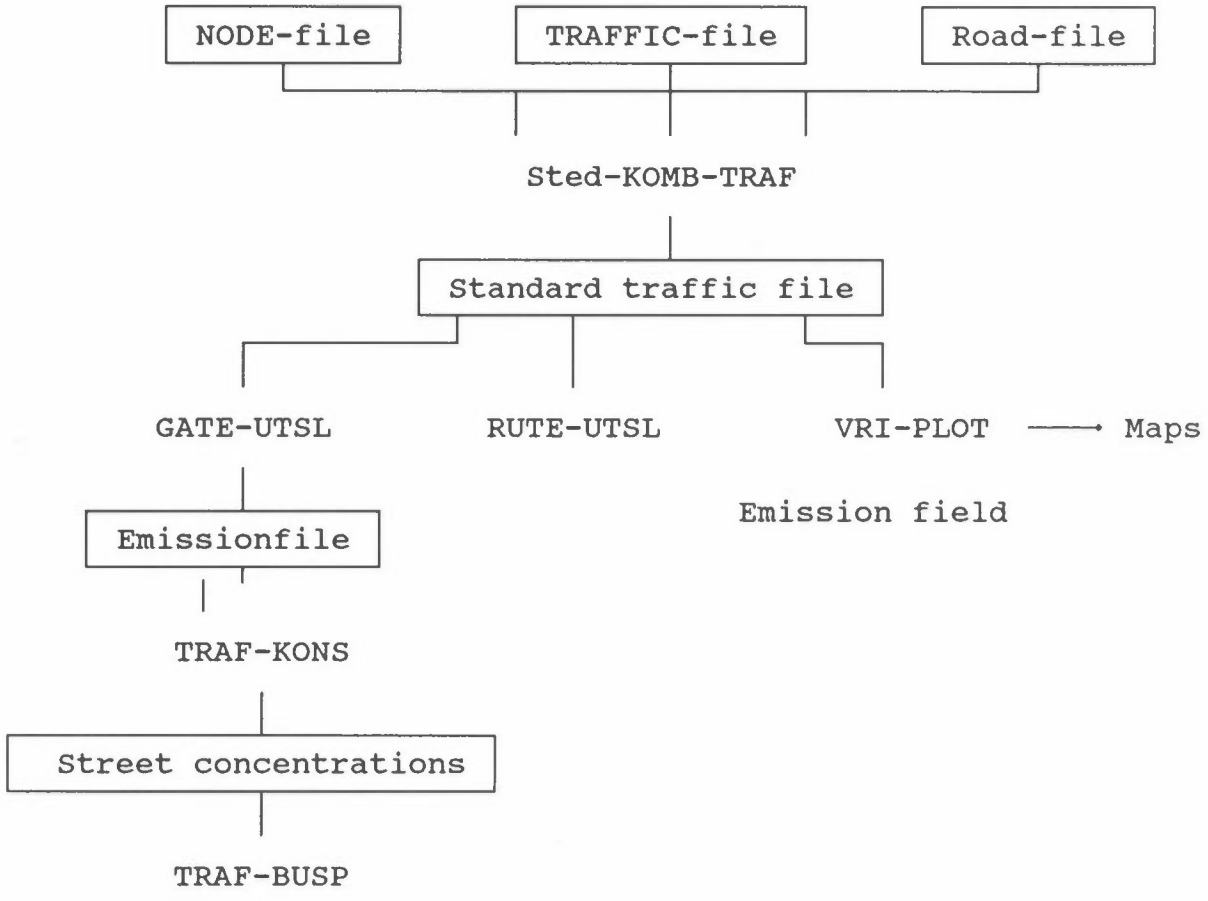

5 CONVERSION OF VEHICLE EMISSION FACTORS TO LINE-SOURCE EMISSION FACTORS FOR ROADS AND ROAD TUNNELS (E-8814)

Dag A. Tønnesen

Different emission factors for different vehicle types at various speeds and accellerations are being put into system to produce line source emission factors for modelling dispersion from roads and road tunnels.

The basis for the emission factors is "Nordisk beregningsmetode for bilavgasser" (NBB, NILU OR 56/84). These vehicle emission

factors are extrapolated for vehicle speeds up to 90 km/h and accellerations from -1.2 m/s^2 to 1.2 m/s^2.

The properties of the actual vehicle classes and numbers, and the fraction of vehicles whose engines are not yet at optimal working temperature, are considered in producing line source emission factors.

The model development will continue in 1990.

6 DISPERSION MODELS FOR ROAD TUNNEL OUTLETS (E-8931)

Dag A. Tønnesen

The purpose of this project is to improve the currently operative road tunnel models at NILU. The following areas are being considered:

- Better description of the different phases of the tunnel jetstream.
- Better description of the extension of the tunnel jetstream.
- Include of the effects of different wind directions relative to the direction of the tunnel jetstream.
- Receptor based concentration calculations.
- Include a simple parameterization of the oxidization of NO to NO_2 so that a total NO_2 concentration can be calculated at specified receptor locations.

The work on the items mentioned above will be undertaken in 1990.

7 VERTICAL DISPERSION OF AIR POLLUTANTS IN A CITY (E-8613)

Knut E. Grønskei

7.1 INTRODUCTION

To improve the description of dispersion of emissions below the height of about 50 m, tracer experiments were performed in urban and suburban areas in Norway. A tentative method to include the dispersion effect of roughness elements was suggested (Grønskei, 1989).

Based on results of further dual tracer experiments the dispersion effect of roughness elements had to be described in further details. A framework of formulae described in chapter 7.2 are used in chapter 7.3 for the descriptions of results of dual tracer experiments.

Measurements by a sonic anemometer are used for the description of turbulence in four dual tracer experiments. Each experiment is carried out as consecutive tests giving two 15 min average samples.

7.2 DISPERSION OF POLLUTION CLOSE TO THE GROUND

Statistical turbulence theory and a description of the meandering process may be used to describe the horizontal dispersion. In this study the vertical dispersion is considered by using parameters describing crosswind integrated profiles.

Wind and turbulence characteristics vary with height and this variation may determine the variation in σ_z-values with distance.

Close to the source, however, it is expected that

$$\frac{d\sigma_z}{dx} = \frac{\sigma_w}{u}$$

The geometry of the roughness elements may determine the structure of the turbulent surface layer, influencing dispersion. Perry et al. (1969), however, described two types of turbulent boundary layers observed above rough walls in a wind tunnel. In the atmosphere the conditions are complicated further by thermal effects and inhomogeneous heat sources introduced by the roughness elements.

K-theory provides a simple framework for studying inhomogeneous dispersion of an inert tracer when the tracer fluctuations are uncorrelated with turbulent fluctuations. The dispersion may be described by solving an equation for the gradient transfer by numerical methods for emissions close to the ground (Gryning et al., 1983). The following simplification applies when wind shear effects are of minor importance, and results of the dispersion experiments may be interpreted in terms of the following differential equation for the first moment ($\bar{z}$) in the vertical concentration distribution (Grønskei, 1989). The equation is written in standard notation.

$$\bar{z}\,\frac{d\bar{z}}{dx} = \lambda(z)\;C_D^{0.5}(\bar{z}) - \frac{\pi-2}{\pi}\,\lambda(z_1)\;C_D^{0.5}\;(z_1) \qquad (1)$$

$$C_D \equiv \left(\frac{u_*}{\bar{u}}\right)^2,\quad \lambda \equiv \frac{K_z}{u_*} \text{ and } \sigma_z = \sqrt{\frac{\pi}{2}}\cdot\bar{z}$$

According to the surface layer similarity theory for stable conditions:

$$C_D^{0.5} = \frac{0.36}{\ln\left(\frac{z}{z_0}\right) + 4.7\left(\frac{z}{L}\right)} \qquad (2)$$

where:

z_0 : surface roughness length.
L : Monin Obukhov length.

The form of Eq. (1) favours some aspects of applications:

- The asymptotic behaviour of dispersion formulae based on statistical theory is preserved.
- The form of several empirical dispersion formulae are maintained as solutions of the simple differential equation.
- The solutions of the differential equation includes additive and multiplicative qualities that facilitate practical application when dispersion conditions varies along air trajectories.

The scale of turbulence cannot be measured on a routine basis, and the theory for the structure of the atmosphere has to be applied.

In the description of second order equations given by Mellor and Yamada (1976) three scales of turbulence are used, one to account for spatial inhomogeneties in covariances between velocity components λ_1, one to account for spatial variations in temperature fluctuation intensities λ_2 and one to account for spatial variations in the transport of heat λ_s.

During stable atmospheric conditions we have been particularly concerned with the effect of the buoyancy term and with spatial variations in the heat transport terms.

To compare experimentally determined dispersion as a result of emission of two tracer components at different heights above the ground (O,H), scaled concentrations are defined in the following way:

$$S = \frac{c \cdot u}{Q} \qquad (3)$$

When Gaussian formulae are used to describe the dispersion of both tracer components, the emission height of the elevated source may be expressed by the two scaled maximum concentrations at ground level:

(Sm (X,0,H), Sm (X,0,0))

The following formula is found for the emission height H.

$$H=\sqrt{2}(1+f)\ \sigma_z{}^0\left[-\ln(1+f)\ \frac{1}{A}\ \frac{Sm(X,0,H)}{Sm(X,0,0)}\right]^{0.5} \qquad (4)$$

$$f \equiv \frac{\sigma_z{}^H - \sigma_z{}^0}{\sigma_z{}^0},\quad A = \frac{\sigma_y{}^0}{\sigma_y{}^H}$$

Index 0 refers to the ground level emission.
Index H refers to the evaluated emission.

When concentration profiles in the vertical direction are not observed, the equation above may offer useful information interpreting dual tracer data to discuss variation in dispersion conditions with height.

7.3 RESULTS OF THE TRACER EXPERIMENTS IN THE LILLESTRØM AREA

The experiments were carried out in a flat residential area with 6 to 10 m high buildings and trees. A dual tracer system was used in which sulphur hexafluoride (SF_6) was released from a mast 36 m above the ground and bromtrifluormethane ($CBrF_3$) was released from ground level (1 m). Each experiment consisted of two sequential 15-min periods. The meteorological measurements were carried out along the 36 m high mast. For further information, see Haugsbakk and Tønnesen (1989).

Table 1 presents average meteorological data for each dispersion experiment. The automatic weather station provides data average for each 5 minutes periods. Three of the experiments were carried out during inversion conditions. The wind speed was below 1 m/s in two experiments.

Table 1: Meteorological conditions in tracer experiments.

Date	Time	φ_{36}	$\bar{u}_{36}$	φ_{10}	u_{10}	T_{10}	ΔT_{36-10}	$\sigma \Delta T$
		deg	m/s	deg	m/s	^0C	^0C	^0C
87.01.10	0930-0945	36	4.4	35	2.1	-25.5	-0.1	0.2
	0945-1000	25	3.6	19	1.4	-25.5	-0.2	0.1
87.01.12	0930-0945	34	3.0	60	1.1	-20.5	1.3	0.2
	0945-1000	35	3.1	62	1.0	-20.5	1.3	0.2
87.01.17	1000-1015	331	0.7	329	0.3	-21.2	1.5	0.4
	1015-1030	327	0.8	332	-	-21.1	1.3	0.5
87.02.09	1000-1015	300	0.5	-	-	-12.8	0.2	0.3
	1015-1030	294	0.2	-	-	-12.2	0.5	0.4

$\varphi_{36}, \varphi_{10}$: wind direction at 36 m and at 10 m above ground level
$\bar{u}_{36}, u_{10}$: wind speed at 36 m and at 10 m above ground level
T_{10} : temperature at 10 m level
ΔT_{36-10}: temperature difference between 36 m and 10 m level
$\sigma \Delta T$: the standard deviation of the temperature difference readings.

Sonic anemometer measurements were processed to give 10 min average values for wind speed and wind directions at 10 m level, further covariances between velocity components and between velocity components and temperature fluctuations were given.

Table 2 shows parameters measured by a sonic anemometer to characterize atmospheric turbulence. It is seen that the covariances between the fluctuations in the velocity components varies with the wind speed and that fluctuations occur between the two consecutive 15 min periods in an experiment.

Values for the drag coefficient and for the Monin Obukhov length are presented in Table 3. The observed values are compared with calculated values. The calculations are based on surface layer theory using data for wind and temperature structure.

Table 2: The atmospheric turbulence during tracer experiments. Standard notation is used.

Date	Time	q*	$\overline{w'^2}$	$\overline{v'^2}$	$\overline{u'w'}$	$\overline{w'T'}$	$\bar{u}_{10}$	$\frac{\Delta\theta}{\Delta z}$	$\sigma_w/\bar{u}$
		10^{-2} m^2/s^2	10^{-2} m^2/s^2		10^{-2} m^2/s^2	m/s ^0C	m/s	10^{-2} $^0C/m$	
870110	0930-0945	117	22	38	-14	-14	2.1	0.8	0.22
	0945-1000	87	18	29	- 8	-11	1.7	0.6	0.25
870112	0930-0945	35	5	10	- 3	-13	1.7	6.1	0.13
	0945-1000	31	5	10	- 3	-10	1.6	6.0	0.14
870117	1000-1015	10	1	6	- 5	0.5	0.9	6.9	0.11
	1015-1030	8	1	3	- 1	- 0.3	0.5	5.8	0.20
870209	1000-1015	10	3	3	- 1	7	0.5	1.7	0.35
	1015-1030	9	2	5	0	6	0.4	2.8	0.35

*: $q \equiv \overline{u'^2} + \overline{v'^2} + \overline{w'^2}$

Table 3: Drag coefficient and Monin Obukhov length.

Date	Time	$C_{DF}^{0.5}$	$C_{DS}^{0.5}$	L_F	L_S
870110	0930-0945	0.18	0.09	235	56
	0945-1000	0.16	0.09	130	74
870112	0930-0945	0.10	0.08	27	9.4
	0945-1000	0.12	0.08	41	6.4
870117	1000-1015	0.26	<0.1	-1601	0.1
	1015-1030	0.19	<0.1	188	0
870209	1000-1015	0.20	<0.1	-8.1	0.2
	1015-1030	-	<0.1	-	-

$C_{DF} = \left(\frac{-\overline{u'w'}}{u^{2-}}\right)$ Sonic anemometer data.

$C_{DS}^{0.5} = \frac{0.36}{\ln \frac{z}{z_0} + 4.7 \frac{z}{L}}$ Surface layer theory.

$L_F = -\frac{u'^3 T}{g k \overline{w'T'}}$ Sonic anemometer data.

L_S : Using surface layer theory and obserservations of vations of variation with height of wind and temperature to determine Monin Obukhov length.

The vertical exchange of momentum observed at the level of 10 m is larger than expected from surface layer theory. As a result both the drag coefficient C_D and the Monin Obukhov length L are larger than expected from surface layer theory.

Table 4 shows results of the tracer experiments. The σ_y-values are determined from observed pollution traverses as the best fit to a Gaussian pollution distribution with σ_y as standard deviation and C_C as maximum concentration value. C_0 is the observed maximum along the traverses.

Table 4: Results of dual tracer experiments.

Date	Time	X	$CBrF_3$				SF_6			
			C_0	C_C	σ_y	σ_z	C_0	C_C	σ_y	H
			$\mu g/m^3$	$\mu g/m^3$	m	m	$\mu g/m^3$	$\mu g/m^3$	m	m
870110	0930-0945	160	55.3	45.8	49	7.0	7.6	6.7	65	15
		490	5.9	5.5	108	26.5	4.8	3.2	129	39
		810	3.0	2.1	145	52.2	3.7	2.9	144	48
	0945-1000	140	68.9	65.6	50	4.7	8.3	8.6	54	11
		440	8.1	6.6	114	21.2	5.2	3.4	132	36
		820	3.1	2.5	220	28.7	3.4	2.5	237	38
870112	0930-0945	150	130	119	55	2.2	11.1	8.6	49	5
		300	31.2	23.3	96	7.0	2.7	2.6	68	18
		460	18.9	16.5	125	7.7	2.3	2.2	115	19
	0945-1000	160	198	172	57	0	8.6	7.6	52	-
		300	47.6	42.3	71	5.2	5.8	5.1	58	17
		440	15.2	13.6	145	8.0	2.8	2.7	113	19
870117	1000-1015	150	93.6	77.5	50	16.3	6.9	6.1	41	44
		470	14.6	13.0	120	40.4	3.3	2.0	98	100
		900	10.8	9.9	126	50.7	7.6	8.2	134	52
	1015-1030	150	158	154	84	4.8	1.7	1.5	69	16
		490	17.5	11.6	133	41.0	6.2	5.8	79	84
		900	10.3	9.8	148	43.5	5.8	4.0	131	86
870209	1000-1015	190	45.1	39.3	105	15.4	29.6	24.9	55	31
		410	11.5	9.9	107	59.4	9.7	9.9	95	85
	1015-1030	190	69.5	53.5	117	10.1	45.8	35.8	59	20
		430	23.8	20.7	102	29.9	20.0	19.4	98	43

From the requirement of mass consistency for the $CBrF_3$ emissions from 1 m level, the σ_z-values were determined.

For the SF_6 emission from 36 m level it was necessary also to consider the height of the plume above the ground to explain the observed concentration values. The H-values in the table are calculated using equation 4 assuming A=1 and f=0.

The σ_z-values shown for the ground level emission in Table 4 are used to define the left hand side of equation 1. The results indicate that for the experiments carried out on 12 January and on 17 January, the right hand side of the equation approach a constant value. Using the observed values of C_0 the scale of turbulence was estimated to be 1.1 and 1.3 m respectively. When the scale of turbulence is estimated by the method suggested by Venkatram et al. (1984) larger values are found indicating more effective vertical dispersion.

Using the method of dispersion classification that has been suggested by Holtslag et al. (1985) it is found that for the experiments carried out on the 10 and on the 12 January the elevated source was just above the stable surface layer.

Weak winds are observed on the 17 January and on the 9 February. When data on the wind and temperature stratification in the atmosphere are used, it is found that the experiments took place under conditions that were not well defined. In table 3 it is seen that the flux determined Monin Obukhov length varied with time. Observations of 5 min average wind speed and direction further show that the meandering of the wind became important.

Figure 2 shows that for ground level emission in the surface layer, good correspondence between observed and calculated values are found in the stable surface layer calculations. The calculated values are based on the model developed by Gryning et al. (1983). Maximum SF_6 concentration occur closer to the

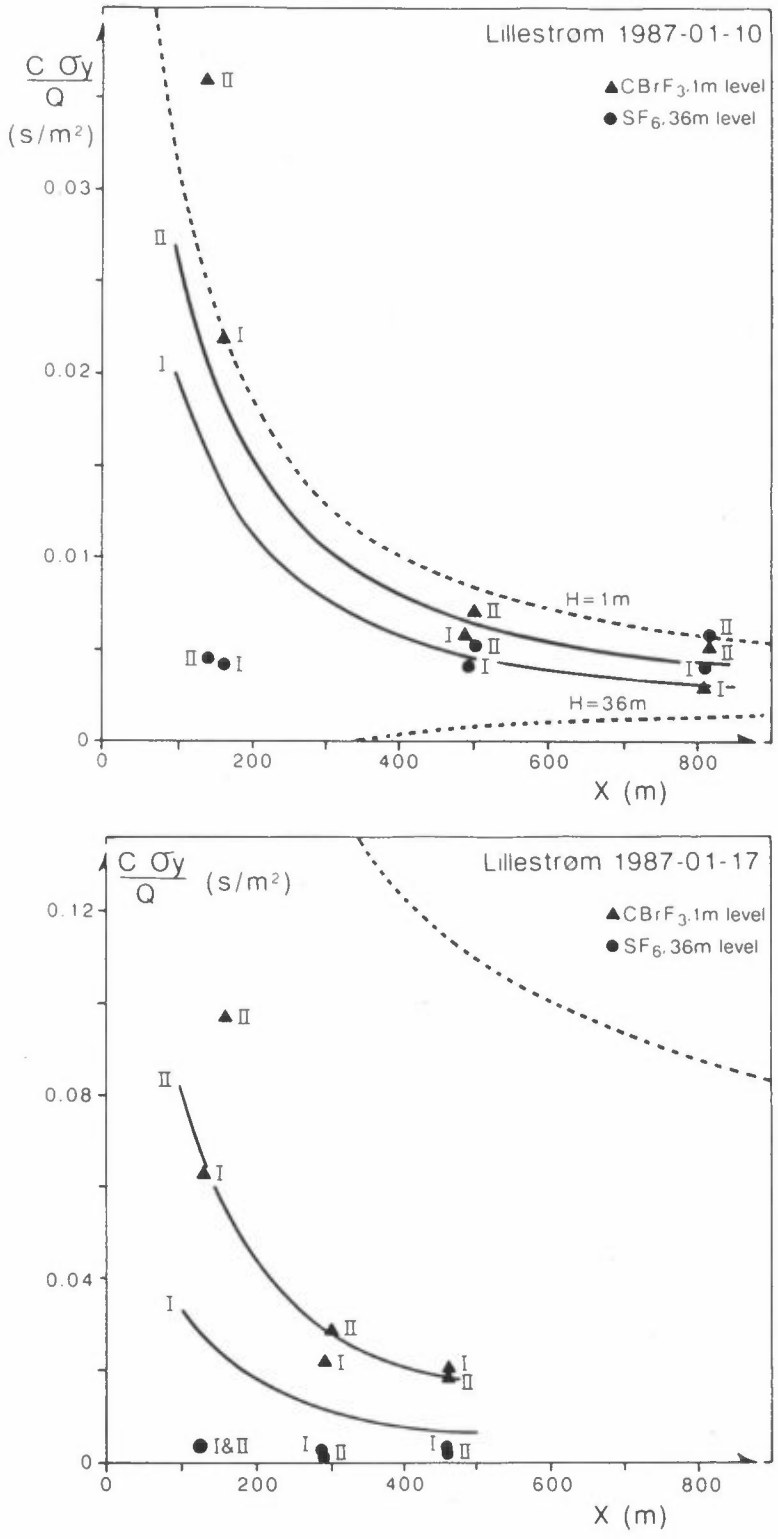

Figure 2: Scaled ground level concentration values in two sequential 15-min periods (I and II). The values are given as function of distance from the source. Calculated values based on turbulence observations are shown by solid lines. Calculated values based on wind and temperature profile observations are shown by broken lines.
a) Tracer experiment on 10 January 1987.
b) Tracer experiment on 17 January 1987.

source than expected, a typical result in all experiments carried out over Lillestrøm in stable atmospheric situations.

In low wind conditions surface layer calculations based on data for wind and temperature variation with height overestimated observed concentrations. When data for observed turbulence is used, correspondence between observed and calculated values is found.

7.4 CONCLUDING REMARKS

Turbulent fluxes of momentum, measured by a sonic anemometer 10 m above ground level, were larger than expected from surface layer theory yielding a large drag coefficient.

In weak wind situations it was a tendency for positive covariance between vertical motion and temperature fluctuations. As a result negative Monin Obukhov length could be observed during inversion situations.

Results of dual tracer experiments indicate that in the stable atmospheric surface layer dispersion equations described dilution from ground level sources well when the wind speed was above 1 m/s, in particular when observed turbulent fluxes of momentum and heat were used for the calculations. In weak wind condition the dispersion calculations based on surface layer theory seriously overestimated the tracer concentrations from a ground level emission. When observed turbulence fluxes were used for dispersion calculations, reasonable correspondence between calculated and observed tracer concentrations was found.

Crosswind integrated tracer concentration as a result of emission above the stable surface layer often indicate that the elevated plume heights are lower than the height of emission.

REFERENCES

Gryning, S.E., Van Ulden, A.P. and Larssen, S. (1983): Dispersion from a continuous ground-level source investigated by a K model. Quart. J. Roy. Meteorol. Soc., 109, 355-365.

Grønskei, K.E. (1989): Description of vertical dispersion influenced by roughness elements. In: Air pollution modelling and its application VII. Ed. Han van Dop. Plenum Press, New York, 1989, pp. 223-235.

Haugsbakk, I. and Tønnesen, D.A. (1989): Atmospheric Dispersion Experiments at Lillestrøm. 1986-1987 Data report. Lillestrøm, Norwegian Institute for Air Research (NILU OR 41/89).

Holtslag, A.A.M., Gryning, S.E., Irwin, J.S. and Sivertsen, B. (1985): Parameterization of the atmospheric boundary layer for air pollution dispersion models, in "15th ITM on Air Pollution Modelling and its Application", St. Louis 1985.

Mellor, G.L. and Yamada, T. (1974): A Hierarchy of turbulence dosure models for planetary boundary layers. J. of Atm. Sciences, 1791-1806.

Perry, A.E., Schofield, W.H. and Joubert, P.N. (1969): Rough wall turbulent boundary layers. J. Fluid Mech., 37, part 2, 383-413.

Venkatram, A., Strimaitis, D. and Dicristofaro, D. (1984: A semiempirical model to estimate vertical dispersion of elevated releases in the stable boundary layer. Atmos. Environ., 18, 923-928.

ACKNOWLEDGEMENTS

Personnel from Risø National Laboratory in Denmark performed sonic anemometer registrations in Lillestrøm for the period 7 January 1987- 9 February 1987.

8 COMBINED STATISTICAL METHODS AND DISPERSION MODELS (E-8920)

Knut E. Grønskei, Sam E. Walker

8.1 INTRODUCTION

In the Grenland area hourly concentrations have been calculated in a 16x23 km^2-grid for the periods 3 January to 15 March 1988 and 23 April to 24 June 1988.

Figure 3 shows a map of the area of the dispersion calculations. Close to point sources a puff model was employed to describe high local (subgrid) concentrations. Along streets with high traffic a street model was used to take maximum exhaust concentration into account as a contribution to exposure estimates.

Deviation between observed and calculated values at specific receptor points occur and the deviations are attributed to the following sources of error:

1. Sources outside the area.

2. Emission from single sources.

   This source of error may be devided in three parts and accounted for by considering:

   2.1 The description of emission intensity on an hourly basis.

   2.2 The description or determination of the hourly mean position of the plume.

   2.3 The description of plume meandering vertically and horizontally.

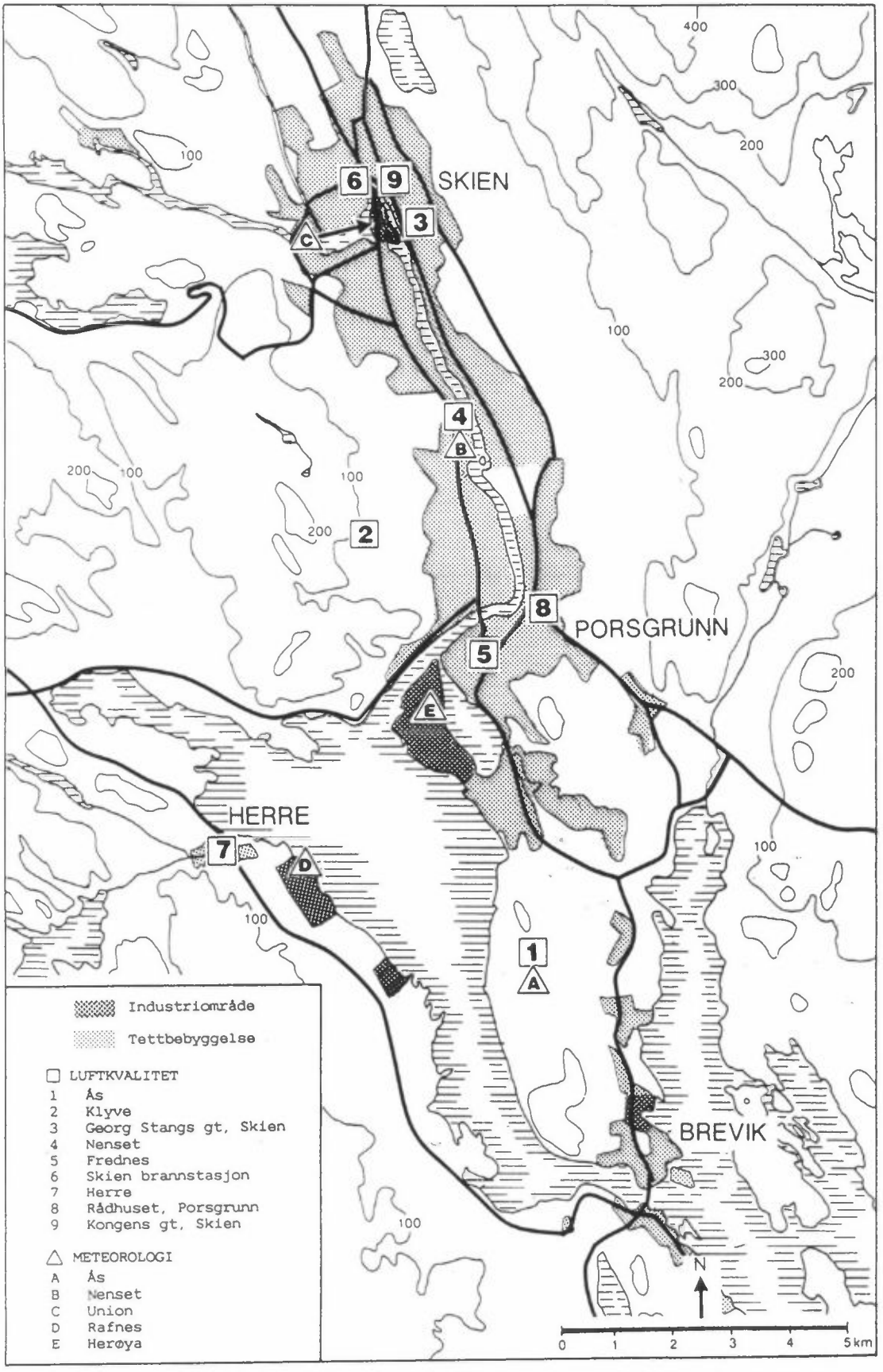

Figure 3: Map of the area of investigation.

3. Emissions from area sources.

   This source of error may be devided in three parts and accounted for by considering:

   3.1 The description of emission intensity on an hourly basis.

   3.2 The description of the spatial concentration distribution.

   3.3 The description of the meandering of the position of pollution distribution.

4. Contribution from a neighbouring single source. This emission may be small and have minor influence on other measuring stations.

The hourly deviations caused by the different sources of errors have different characteristics that can be used in the interpretation of data, i.e.:

Error source 1:
Characterized by an additive correction on all stations.

Error source 2:
Characterized by an influence on measuring station downwind of the emission areas. The area of influence varies with wind and dispersion conditions.

Error source 3:
The contribution from many small low level area sources is characterized by a spatial distribution similar to the spatial source distribution. In this way this source of error influence all measuring stations proportional to the local contribution from the area sources. The factor of proportionality is determined by the conditions of vertical exchange and by emission intensity.

Error source 4:
Should be minimized by considering the neighbourhood of station location. It has to be taken into account as an extended measuring error that limit the applicability of the measurements for interpretation purposes.

From a system of conditional scatter diagrams for NO_x a few scatterplots are shown to identify parts of the model that need to be elaborated.

8.2 RESULTS

Figures 4 and 5 show scatter diagrams with observed versus calculated values during daytime (06-22) when the wind is from west to north (DD $\in$ [270°, 360°]). Figure 4 shows the result for receptor location Nenset and Figure 5 shows the result for Frednes.

The results presented in figures 4 and 5 are interpreted in the following way:

When the error may not be accounted for by a small adjustment in calculated spatial concentration distribution, a systematic underestimation may occur as a result of emission on local roads (see Figures 6 and 7). this is one dominant source of error.

During night time (23-05) when emissions from car traffic are small and when the wind blowing from other directions, overestimated concentrations may occur.

Within the rush hours the errors that may not be accounted for by spatial adjustments of calculated concentration fields, may be classified as overestimation when winds come from local

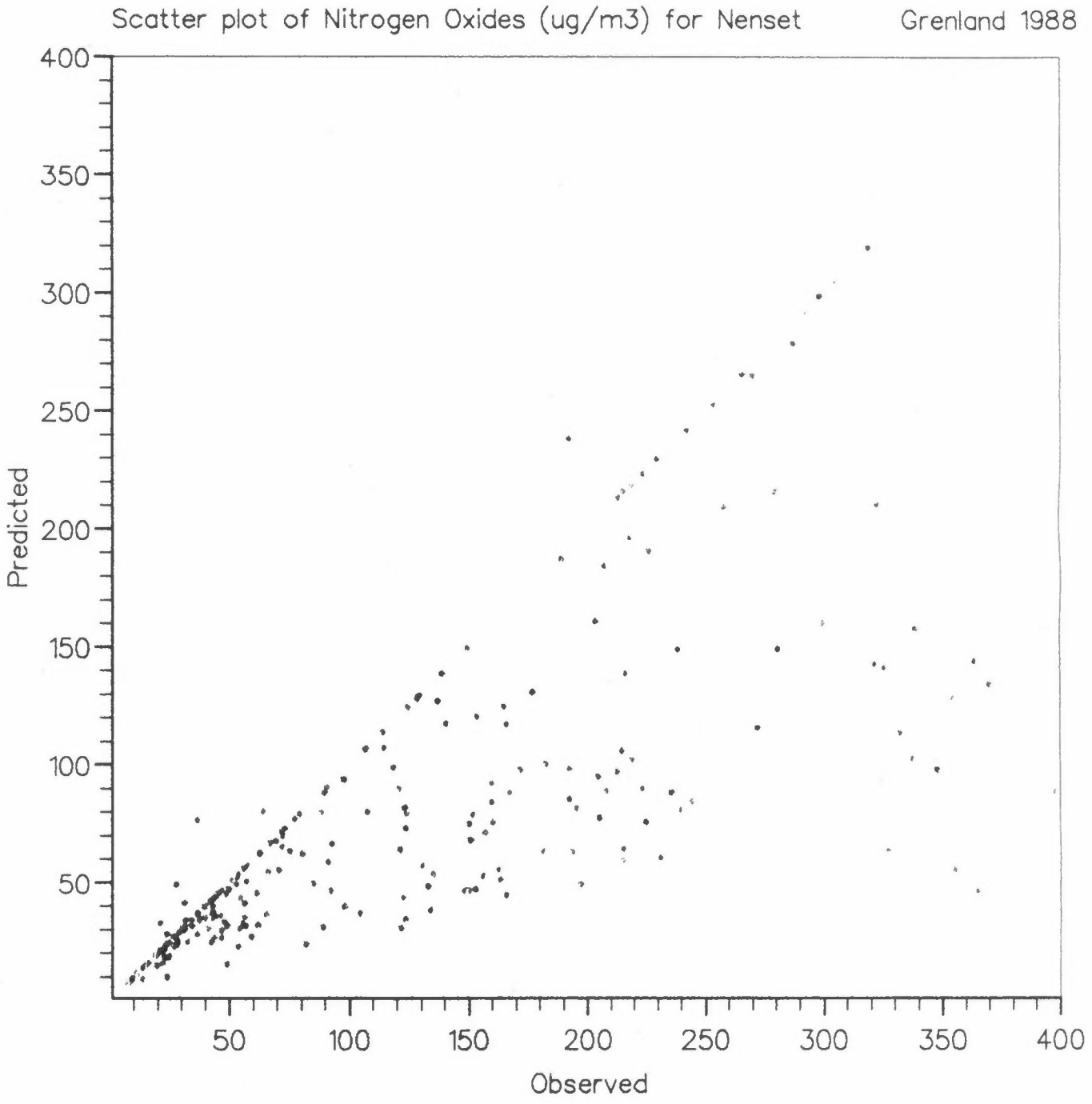

Figure 4: Predicted concentrations as a function of observed values. When corresponding concentration values within a distance of 1 km is found, a point is given on the diagonal corresponding to the observed value. The following conditions are employed selecting hourly values: The hour of the day is between 06 and 22 local wind direction is between 270° and 360°.

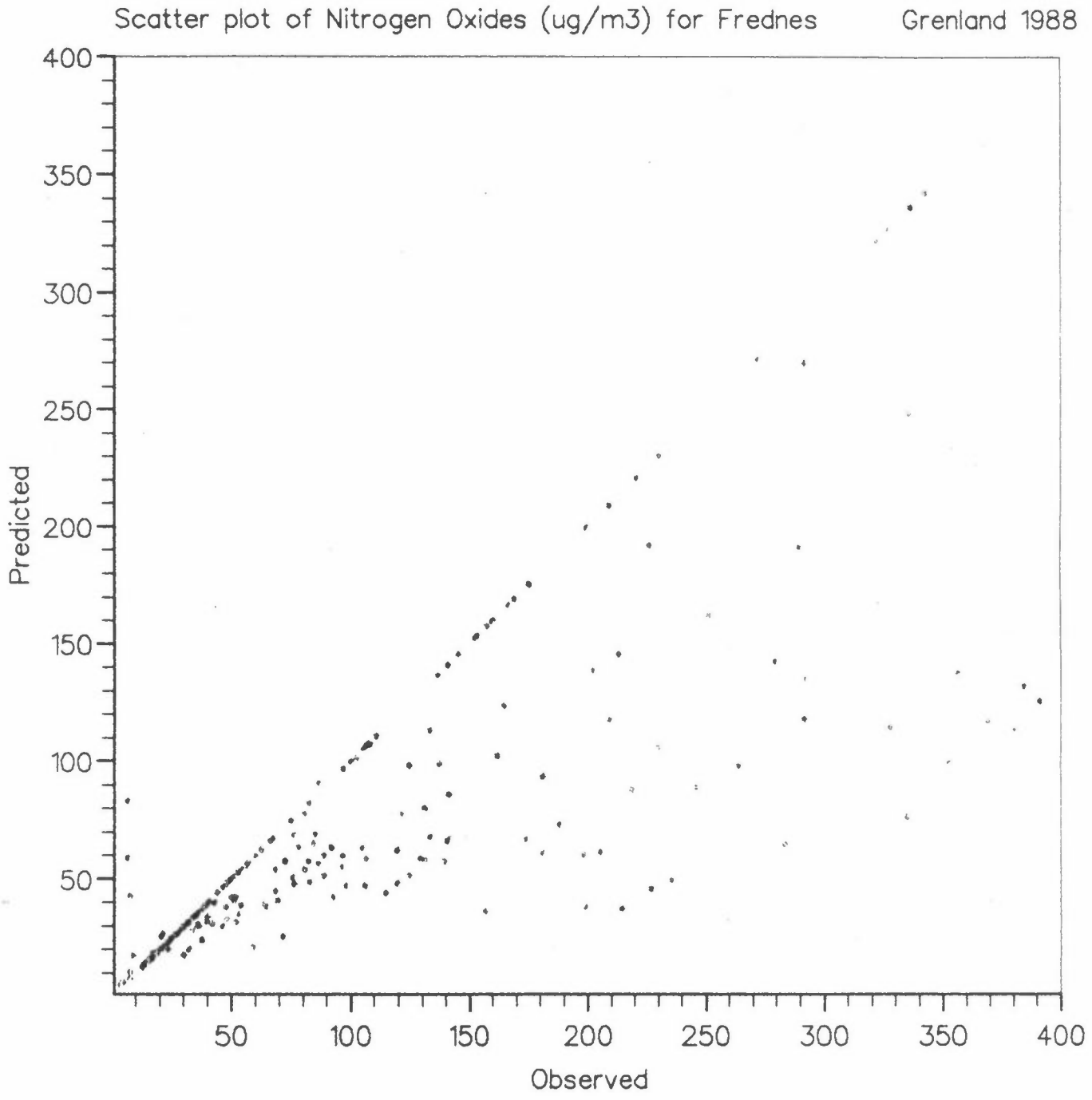

Figure 5: Predicted concentrations as a function of observed values. When corresponding concentration values within a distance of 1 km is found, a point is given on the diagonal corresponding to the observed value. The following conditions are employed selecting hourly values: Hour of the day is between 06 and 22. Local wind direction is between 270° and 360°.

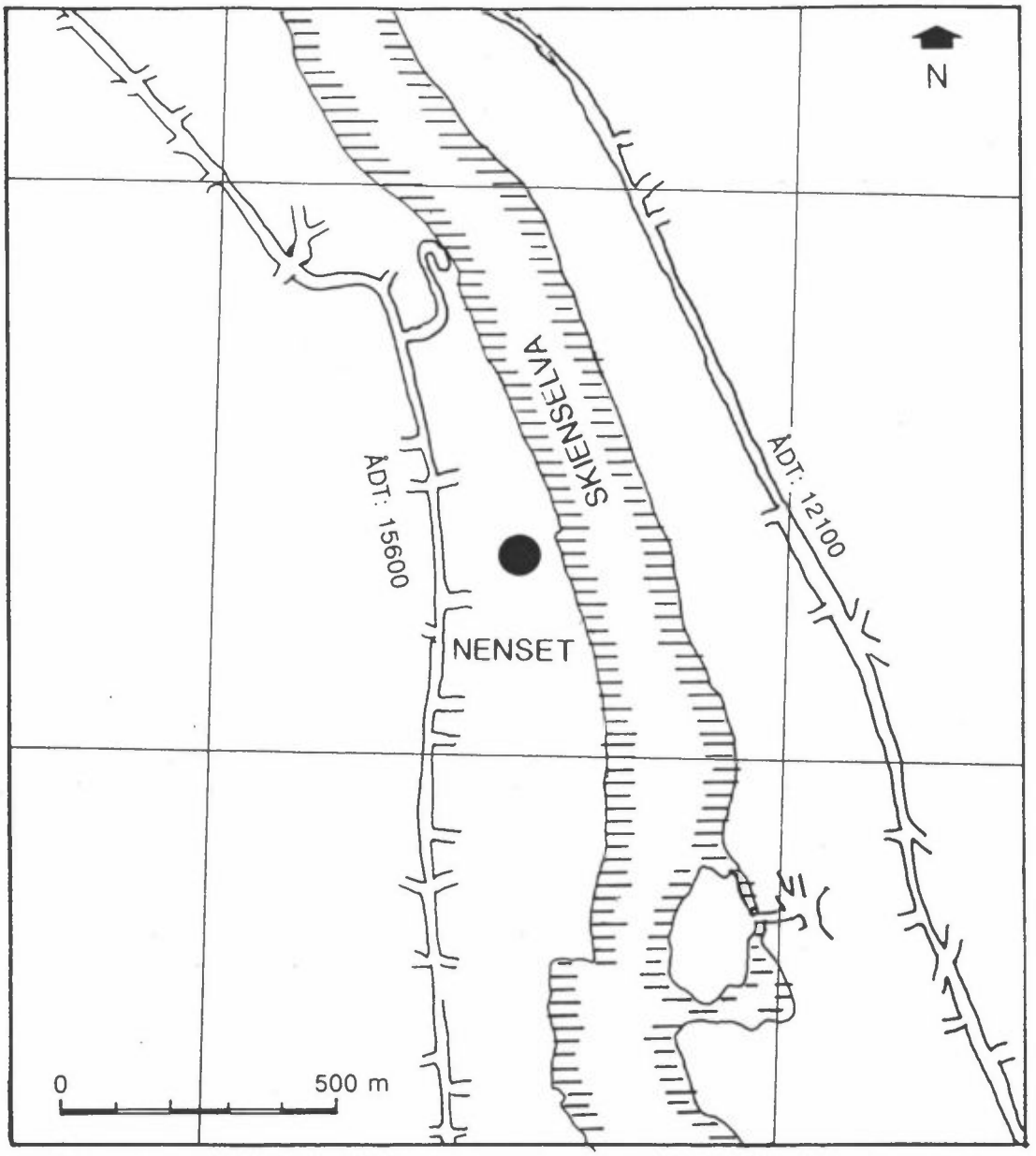

Figure 6: Map of the area and the grid system around the measuring station located at Nenset, Grenland.

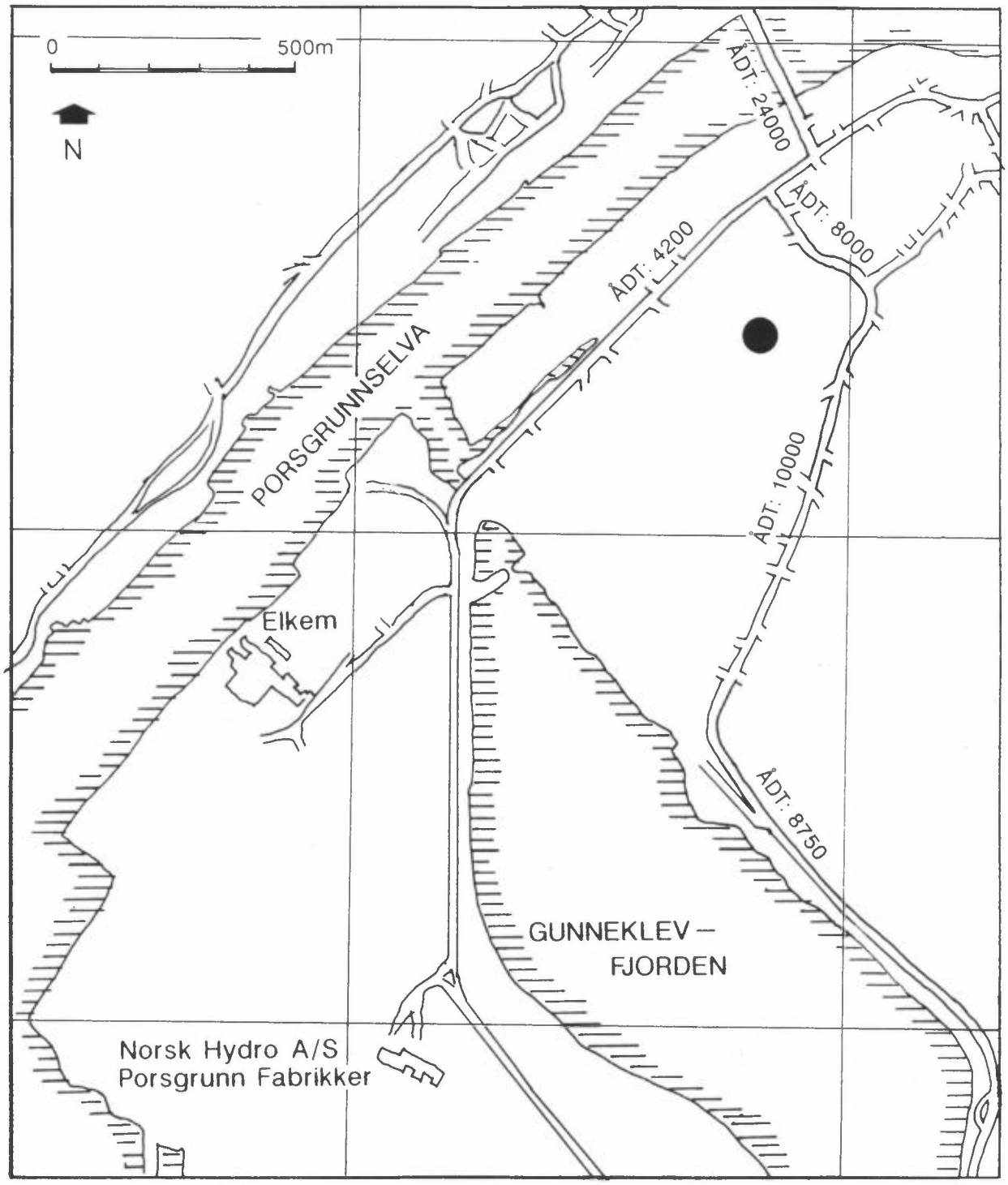

Figure 7: Map of the area and the grid system around the measuring station located at Frednes, Grenland.

roads with high traffic. For small concentrations a tendency for overestimation with wind from southerly direction.

The scatterplot for the stations (Klyve and Aas) exposed to the Herøya area indicate situations with overestimation for wind from the main source area. Winds from other areas are associated with underestimation of observed concentration.

The underestimated values may to some extent be accounted for by background concentrations. The overestimated vallues should be considered by considering the point source mode in more detail.

Considering the scatterplot of daytime concentration and wind from southerly direction, it is a clear tendency to overestimate NO_x concentrations lower than about 60 $\mu g/m^3$ and to underestimate higher concentrations. The same tendency is observed on all measuring stations (see Figures 8-12).

It is a tendency for high concentrations to occur simultaneously with low σ_w-values, low σ_w-values occur simultaneously with high σ_w-values.

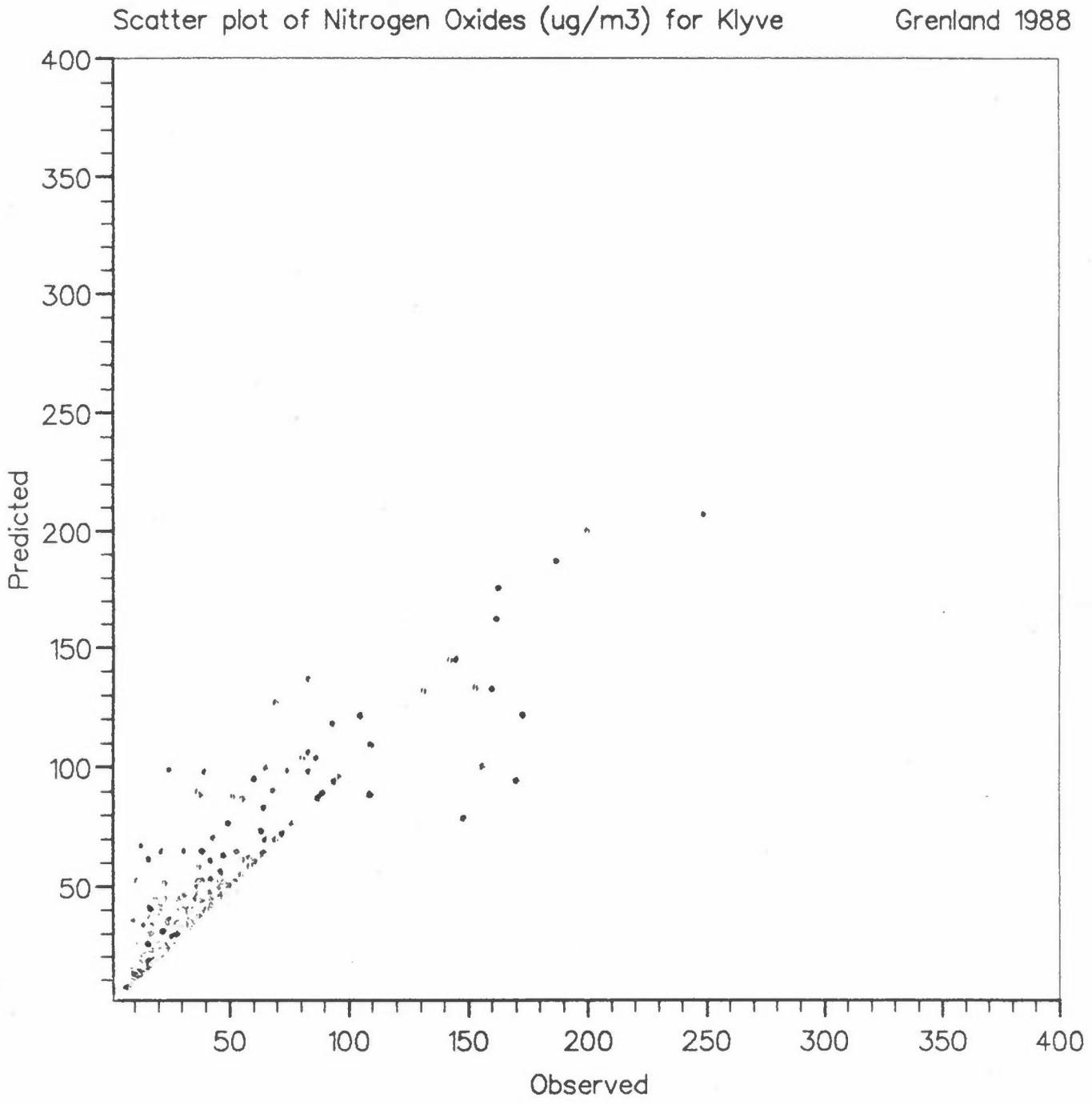

Figure 8: Predicted concentrations as a function of observed values. When corresponed concentration values within a distance of 1 km is found, a point is given on the diagonal corresponding with the observed values. The hour of the day is between 06 and 22. Wind direction is between 90^0 and 270^0 (from southerly direction).

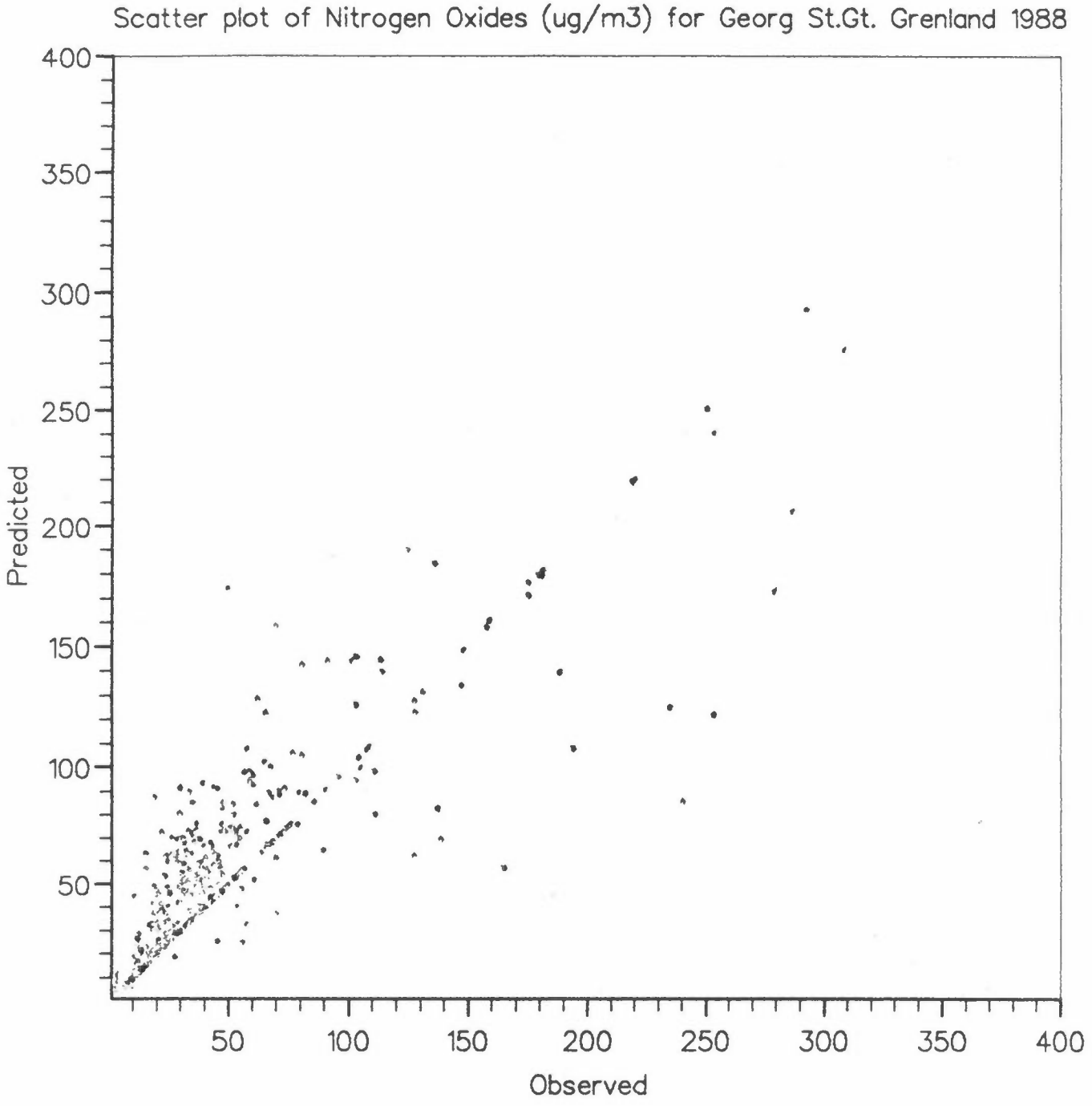

Figure 9: Predicted concentrations as a function of observed values. When corresponed concentration values within a distance of 1 km is found, a point is given on the diagonal corresponding with the observed values. The hour of the day is between 06 and 22. Wind direction is between 90^0 and 270^0 (from southerly direction).

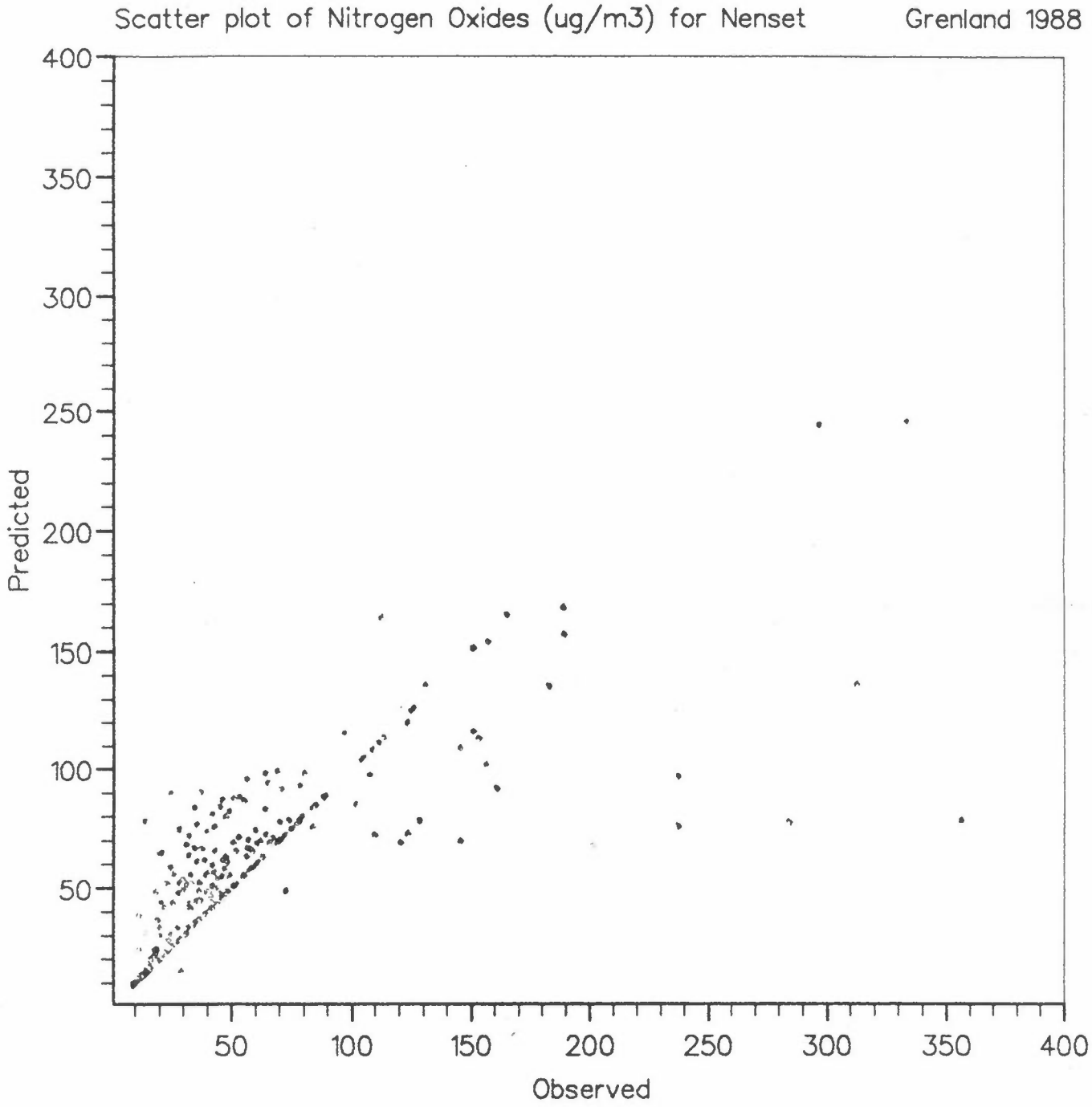

Figure 10: Predicted concentrations as a function of observed values. When corresponed concentration values within a distance of 1 km is found, a point is given on the diagonal corresponding with the observed values. The hour of the day is between 06 and 22. Wind direction is between 90^0 and 270^0 (from southerly direction).

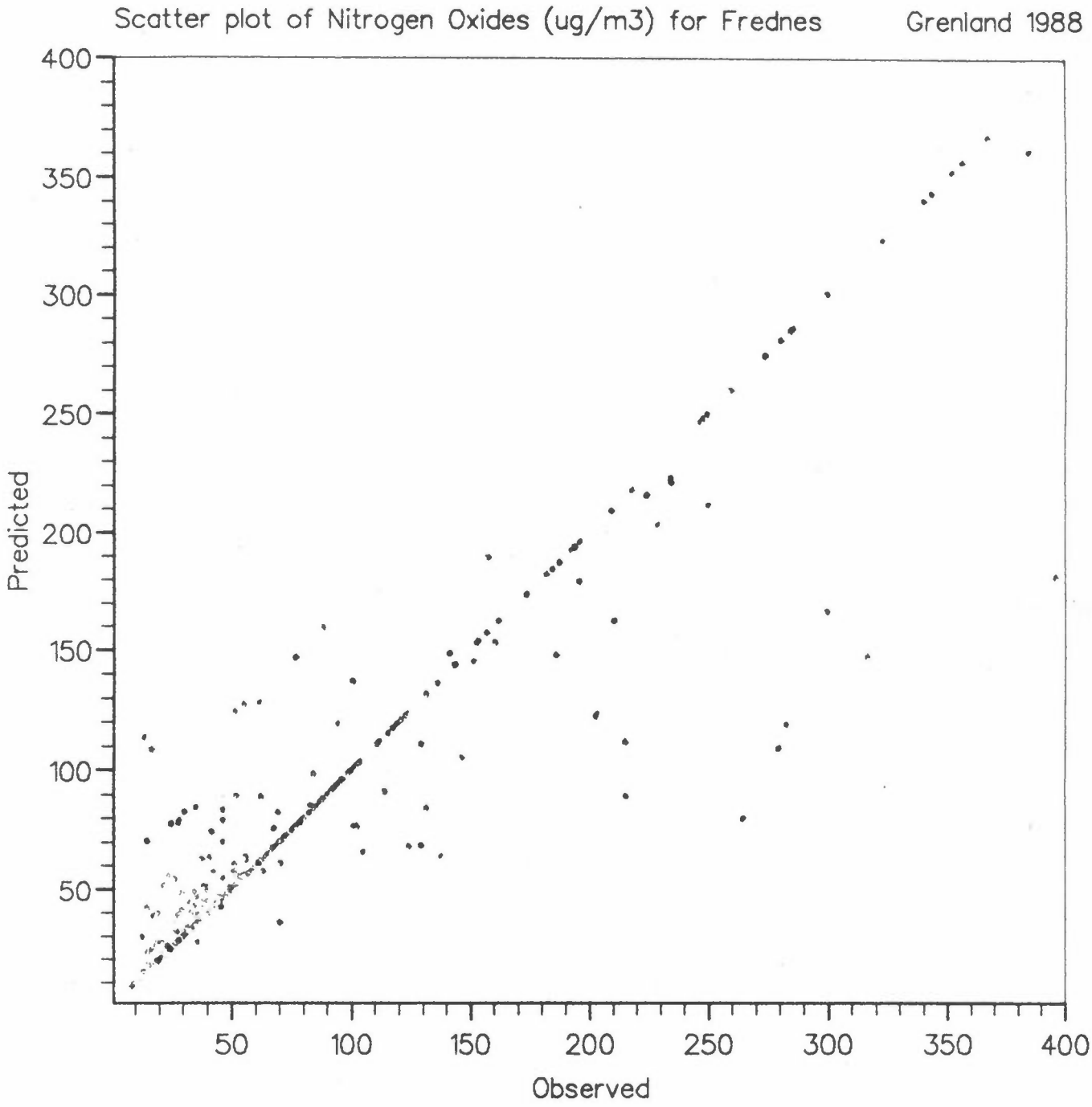

Figure 11: Predicted concentrations as a function of observed values. When corresponed concentration values within a distance of 1 km is found, a point is given on the diagonal corresponding with the observed values. The hour of the day is between 06 and 22. Wind direction is between 90^0 and 270^0 (from southerly direction).

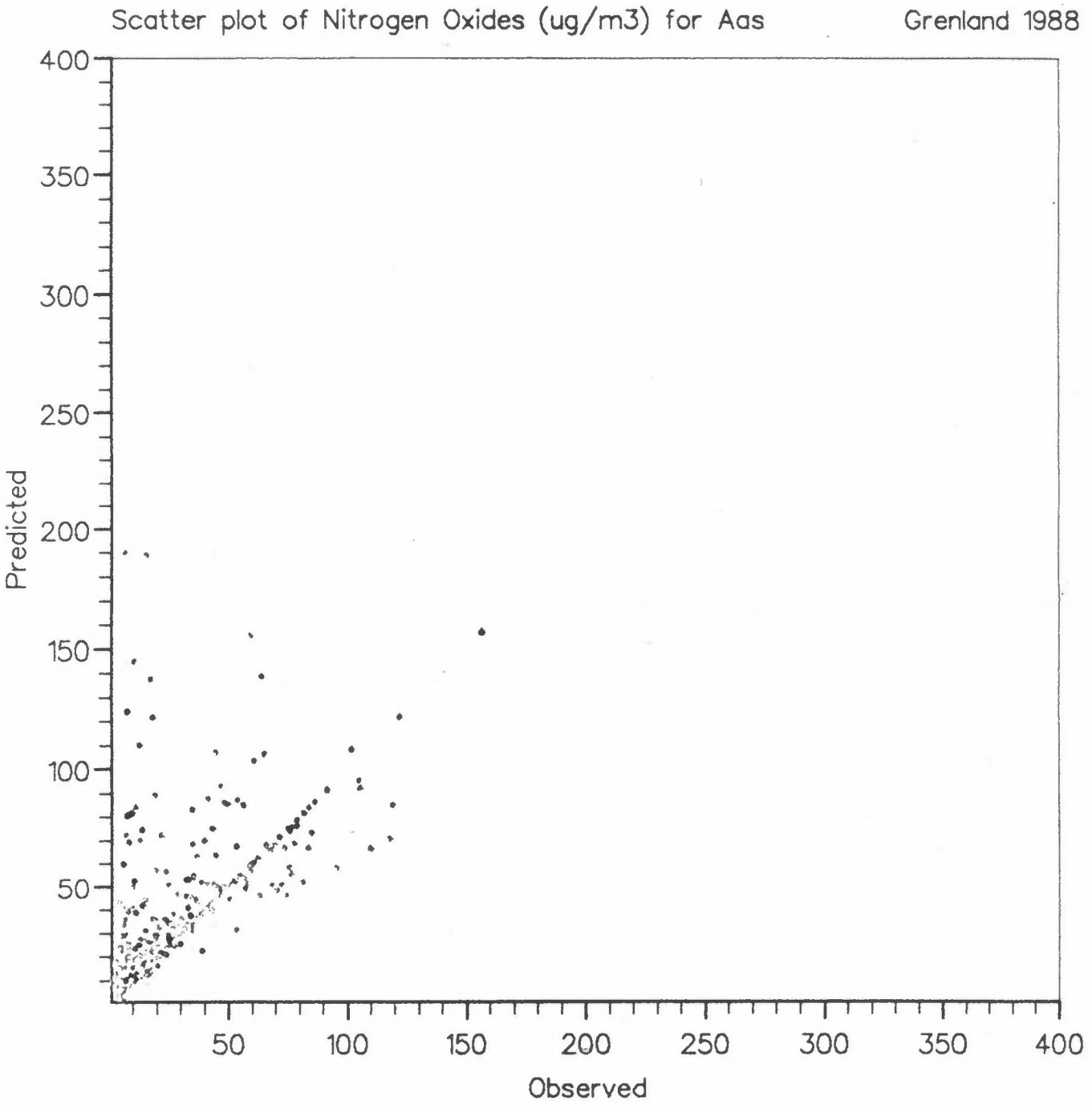

Figure 12: Predicted concentrations as a function of observed values. When corresponed concentration values within a distance of 1 km is found, a point is given on the diagonal corresponding with the observed values. The hour of the day is between 06 and 22. Wind direction is between 90^0 and 270^0 (from southerly direction).

CONCLUDING REMARKS

Conditional scatterplots have been used to identify the most important sources of errors calculating concentration distributions in Grenland. The main discrepancies may be reduced by considering the following model elements:

- Pollution contribution from main roads should be taken into account.

- A tendency to overestimate contribution from main point sources is recorded.

- A larger variability in the description of vertical exchange in the atmosphere should be developed for a better description of the area source contribution.

9 TREATMENT OF METEOROLOGICAL OUTPUT FROM SODAR SYSTEMS (E-8813)

Dag A. Tønnesen

During the last three years NILU has gained experience using Sonic Detecting and Ranging (SODAR) measuring systems.

The output data from the SODAR is quite different from the more conventional windwane cup anemometer equipment usually applied by NILU. As a result of this a new procedure in the treatment of these data must be established.

Data programmes for conversion of fixed axis mean values and standard deviation to polar co-ordinates with transversal and longitudinal standard deviations and for initial data control and structurization have been completed. Improvement in "first-edition" programmes concerning search for special cases and statistical treatment of the output is still needed.

The project was not concluded in 1989.

NORSK INSTITUTT FOR LUFTFORSKNING (NILU)
NORWEGIAN INSTITUTE FOR AIR RESEARCH
POSTBOKS 64, N-2001 LILLESTRØM

RAPPORTTYPE TEKNISK RAPPORT	RAPPORTNR. TR 6/90	ISBN-82-425-0126-2	
DATO MAI 1990	ANSV. SIGN. Hovland	ANT. SIDER 35	PRIS NOK 60,-
TITTEL Research and development within the local air pollution group at NILU Annual report 1989		PROSJEKTLEDER	
		NILU PROSJEKT NR. Q-303	
FORFATTER(E) B. Sivertsen		TILGJENGELIGHET A	
		OPPDRAGSGIVERS REF.	
OPPDRAGSGIVER (NAVN OG ADRESSE) NILU			
3 STIKKORD (à maks. 20 anslag) Modelling | Dispersion | Meteorology			

REFERAT (maks. 300 anslag, 7 linjer)

TITLE

ABSTRACT (max. 300 characters, 7 lines)
The report summarizes some of the research and devleopment conducted by the local air pollution group at NILU during 1989.

A major part of this work was linked to air pollution modelling. Models for various kinds of applications are steadily being improved. New developments were linked to improvements of the description of vertical dispersion, and the improvement of performance through introduction of statistical optimi-zation procedures.

* Kategorier: Åpen - kan bestilles fra NILU A
Må bestilles gjennom oppdragsgiver B
Kan ikke utleveres C